

Distribution and Classification of Peripapillary Retinal Nerve Fiber Layer Thickness in Healthy Young Adults

Gareth Lingham ¹, Samantha Sze-Yee Lee ¹, Jason Charng ¹, Antony Clark ¹, Fred K. Chen ¹, Seyhan Yazar ^{1,2}, and David A. Mackey ¹

¹ Centre for Ophthalmology and Visual Science (incorporating Lions Eye Institute), University of Western Australia, Perth, Australia

² Garvan Institute for Medical Research, Sydney, Australia

Correspondence: Gareth Lingham, Lions Eye Institute, 2 Verdun St, Nedlands WA 6009, Australia. e-mail: garethlingham@lei.org.au

Received: February 17, 2021

Accepted: June 3, 2021

Published: August 3, 2021

Keywords: retinal nerve fiber layer; young adults; epidemiology; classification; the Raine Study

Citation: Lingham G, Lee SSY, Charng J, Clark A, Chen FK, Yazar S, Mackey DA. Distribution and classification of peripapillary retinal nerve fiber layer thickness in healthy young adults. *Transl Vis Sci Technol.* 2021;10(9):3. <https://doi.org/10.1167/tvst.10.9.3>

Purpose: To report the distribution of peripapillary retinal nerve fiber layer (RNFL) thickness in healthy young adults, investigate factors associated with RNFL thickness, and report the percentage of outside normal limits (ONL) and borderline (BL) RNFL thickness classifications based on the optical coherence tomography (OCT) manufacturer reference database.

Methods: Participants of the Raine Study Generation 2 cohort (aged 18–22 years) underwent spectral domain OCT imaging with an RNFL circle scan. Eyes with inadequate scans or optic nerve pathology were excluded. Linear mixed models were used to analyze associations.

Results: Data were available for 1288 participants (mean age, 20.0 years). Mean RNFL thicknesses in right and left eyes, respectively, were global = 100.5 μm , 100.3 μm ($P = 0.03$); temporal = 73.1 μm , 68.9 μm ($P < 0.001$); superotemporal = 140.6 μm , 136.3 μm ($P < 0.001$); superonasal = 104.9 μm , 115.1 μm ($P < 0.001$); nasal = 79.7 μm , 79.1 μm ($P = 0.09$); inferonasal = 109.8 μm , 111.5 μm ($P < 0.001$); and inferotemporal = 143.2 μm , 143.6 μm ($P = 0.51$). Longer axial length was associated with thinner RNFL globally, nasally, inferotemporally, superotemporally, superonasally, and inferonasally, as well as thicker RNFL temporally. The prevalence of ONL and BL classifications was generally higher than the expected rates of 1% and 4%, respectively, in temporal sectors and lower than expected in nasal sectors. The prevalence of global BL classifications was lower than expected (right eye, 2.3%; left eye, 2.6%).

Conclusions: Measured RNFL thickness differs with axial length and between right and left eyes. More reference data are needed to better define the normal limits of RNFL variation in different populations.

Translational Relevance: This study provides an improved understanding of normal variation in RNFL thickness in young adults.

Introduction

Optical coherence tomography (OCT) technology allows retinal nerve fiber layer (RNFL) thickness to be quantified,¹ providing a useful tool for detecting early glaucoma and monitoring its progression.² To aid in interpreting an RNFL thickness measurement, most OCT manufacturers compare a patient's RNFL thickness measurement to an age-matched reference database comprising healthy individuals. An RNFL thickness that is present in the lowest $\leq 1\%$ of values

in the reference population is categorized as outside normal limits (ONL), an RNFL thickness present in $> 1\%$ and $\leq 5\%$ of the lowest RNFL values in the reference population is categorized as borderline (BL), and RNFL thicknesses present in the upper 95% of values in the reference population are classified as within normal limits (WNL).³ Therefore, an appropriate reference database is imperative to ensure accurate classifications. Normative RNFL data from large studies have been published on Australian adolescents⁴ and on older adult populations around the world, such as Beijing,⁵ Singapore,⁶ and Germany⁷; however, data on

the normal distribution of RNFL thickness in young adults are sparse.

The prevalence of myopia is higher among young adults compared to older individuals and is increasing in many parts of the world.^{8,9} Myopia is known to impact measured RNFL thickness^{10,11} and is associated with a higher risk of glaucoma and thus vision loss.¹² To adequately detect thinned RNFL in young adults, it is essential to compare measurements to normative data derived from young adult populations, as extrapolating RNFL thickness distributions from older cohorts may not adequately represent the actual distribution of RNFL thickness.

We aim to describe the normal distribution of RNFL thickness in a population of healthy, young adult Australians; investigate factors that impact the distribution of RNFL thicknesses; and assess the frequency of RNFL thicknesses falling outside the normative range provided by the OCT manufacturer database.

Methods

The Generation 2 (Gen2) cohort of the Raine Study is a birth cohort born between 1989 and 1992. Pregnant mothers, between 16 and 20 weeks of gestation, were recruited into the study through convenience sampling from clinics at a public tertiary antenatal hospital and surrounding private practices as part of a randomized controlled trial on the impact of multiple ultrasounds on fetal growth. Women were eligible for enrollment in the Raine Study if they were expected to deliver at the tertiary antenatal hospital, were sufficiently proficient in English, and intended to reside in Western Australia. There were 2868 live births to mothers recruited into the Raine Study. The Gen2 cohort has been regularly followed up since, including comprehensive eye examinations at the Gen2 20-year follow-up conducted between 2010 and 2012.¹³ An analysis of the representativeness of the Gen2 Raine Study cohort at various follow-ups has been published.¹⁴ At birth, Gen2 Raine Study participants were largely representative of the Western Australian population, but their births were more likely to be complicated or by caesarean. This may be because many participants were recruited from a tertiary antenatal center. At the 20-year follow-up, participants were representative of the broader Western Australian population with the exception that they are less likely to be of Indigenous Australian descent.¹⁴

The Gen2 20-year follow-up was approved by the University of Western Australia Human Research

Ethics Committee, the study adhered to the tenets of the Declaration of Helsinki, and participants provided written informed consent to participate after explanation of the nature and possible consequences of the study. Although the Raine Study is prospective in nature, this is a cross-sectional analysis of the study.

Eye Examination

The protocol for the Gen2 20-year follow-up eye examination has been previously described.¹³ Participants underwent spectral domain OCT (SD-OCT) imaging using the Spectralis HRA + OCT (Heidelberg Engineering, Heidelberg, Germany; acquisition software version 5.1.3.0) according to a standard protocol that included measuring RNFL thickness of both eyes using a circle scan of a diameter of 12 degrees centered on the optic nerve head. Prior to SD-OCT imaging, average corneal curvature values were entered from autokeratometry (ARK501-A; Nidek, Tokyo, Japan). Participants also completed questionnaires on demographics and ocular history and underwent measurement of intraocular pressure (IOP; TA01i; icare, Vantaa, Finland), ocular biometry including axial length (IOLmaster V5; Carl Zeiss Meditec AC, Jena, Germany), and autorefraction (ARK501-A; Nidek).

RNFL thickness was segmented and data were exported using the SD-OCT manufacturer software (Heidelberg Eye Explorer version 1.9.10.0), which includes adjustment for fovea to disc angle. All RNFL circle scans were reviewed for quality, including RNFL layer segmentation, vertical truncation of the scan, positioning of the circle scan, and location of the fovea. All scans were maintained at a signal-to-noise ratio (Q quality score) of 20 dB or more. This threshold was chosen above the normally recommended 15-dB signal as it has been shown to produce repeatable results,¹⁵ and we felt this was a realistic threshold to aim for as young adult eyes often have a better signal-to-noise ratio. Scans were repeated where necessary and if the participant was willing, and segmentation errors were manually corrected where able. This acquisition and reviewing protocol aligns well with the OSCAR-IB quality control criteria¹⁶ for retinal scans; however, good illumination of the fundus was not specifically checked.

Inclusion and Exclusion Criteria

Scans were excluded if optic nerve pathology was present (e.g., optic disc drusen) or if the quality was inadequate. Inadequate scans included those with vertical image truncation, decentred RNFL circle

scan, image granularity, or artifact precluding accurate RNFL segmentation. We included only participants with RNFL data available on at least one eye in the analysis.

To investigate the frequencies of RNFL WNL, BL, and ONL classifications, we matched the parameters of the Heidelberg Spectralis normative database (Heidelberg Spectralis OCT operating manual, article no. 230131-003) by excluding eyes with refractive error $>+5$ diopters (D) or <-7 D, IOP >22 mm Hg, and participants who were not of northern European descent.

Statistical Analysis

Data were summarized using mean and standard deviation (SD) for approximately normally distributed variables and median and interquartile range (IQR) for all other variables. First and fifth percentiles of RNFL thickness were calculated assuming a Gaussian distribution. Where data were available, both eyes of individuals were included in this analysis. Descriptive data on RNFL thickness are presented for each eye separately. To analyze associations with ocular parameters, including RNFL thickness, we used linear mixed models with a random intercept term included for each participant to account for the correlation between eyes. Models were specified as follows: $y_i = \beta_0 + \beta_1 x_1 + u_i$, where y is the outcome (RNFL thickness), β are the coefficients, x_1 is the variable of interest (more variable and coefficient terms were added for multivariable models), and u_i is the random intercept term that varies for each participant (i). Age, sex, ethnicity, smoking status, axial length, and IOP were identified a priori as variables potentially associated with RNFL. The P value for significance was set at 0.05, but a Bonferroni correction was applied when investigating associations between demographic and ocular parameters and RNFL thickness in each of the seven RNFL sectors, separately, to account for multiple testing (Bonferroni-corrected P value threshold = 0.007). Heteroscedasticity was assessed from residual versus fitted plots. When investigating the frequency of WNL, BL, and ONL RNFL thickness classification, the prevalence and confidence intervals (CIs) for each of the WNL, BL, and ONL classifications were calculated for each RNFL sector: global, nasal, superonasal, inferonasal, temporal, superotemporal, or inferotemporal. To account for multiple testing (seven tests), a Bonferroni correction ($1 - (0.05/7)$) was applied and 99.3% CIs were adopted.

Frequency tables and weighted κ statistics (evenly spaced weights) were calculated to compare the agreement between the manufacturer database RNFL thick-

ness classification and RNFL thickness classification developed based on first and fifth centiles of RNFL thickness in this study and RNFL thickness classifications in the right versus the left eye.

Analyses were conducted in R version 4.0.3 (R Foundation for Statistical Computing, Vienna, Austria).

Results

A total of 1344 Raine Study Gen2 participants underwent an eye examination. Of these, 1302 (97%) participants had a SD-OCT RNFL scan on at least one eye. [Figure 1](#) shows the number of participants with OCT data and number of scans that were excluded and reasons they were excluded. After excluding scans of poor quality, poor centration or segmentation, or eyes with optic nerve pathology, RNFL data were available for 1288 (95.8%) participants: 1224 (95.0%) participants had OCT scans of both eyes, 31 (2.4%) had only right eye scans, and 33 (2.6%) had only left eye scans. The characteristics of the included participants are shown in [Table 1](#). There were no significant differences in RNFL thickness between the Raine Study intervention group (repeat ultrasounds during gestation) and the control group (ultrasounds per standard practice) at the Bonferroni-corrected level of significance of $P < 0.007$ (Supplementary Table S1).

Distribution of Peripapillary Retinal Nerve Fiber Layer Thickness

The distributions of peripapillary RNFL thickness in the global and each of the six RNFL sectors are displayed for each eye separately in [Figure 2](#), and [Table 2](#) shows the mean, SD, and first and fifth percentiles. There were significant differences in RNFL thickness between eyes; RNFL in the right eye was thicker in the global, temporal, superotemporal, and nasal sectors but thinner in the superonasal and inferonasal sectors compared to the left eye.

Factors Associated with Peripapillary RNFL Thickness

Demographic and ocular parameters associated with RNFL thickness are shown in [Table 3](#). Males had a slightly thinner global RNFL thickness on average and significantly thinner RNFL in the temporal and inferotemporal sectors. Older age was associated with a thicker inferonasal and thinner superonasal RNFL. Mean RNFL thicknesses were not significantly

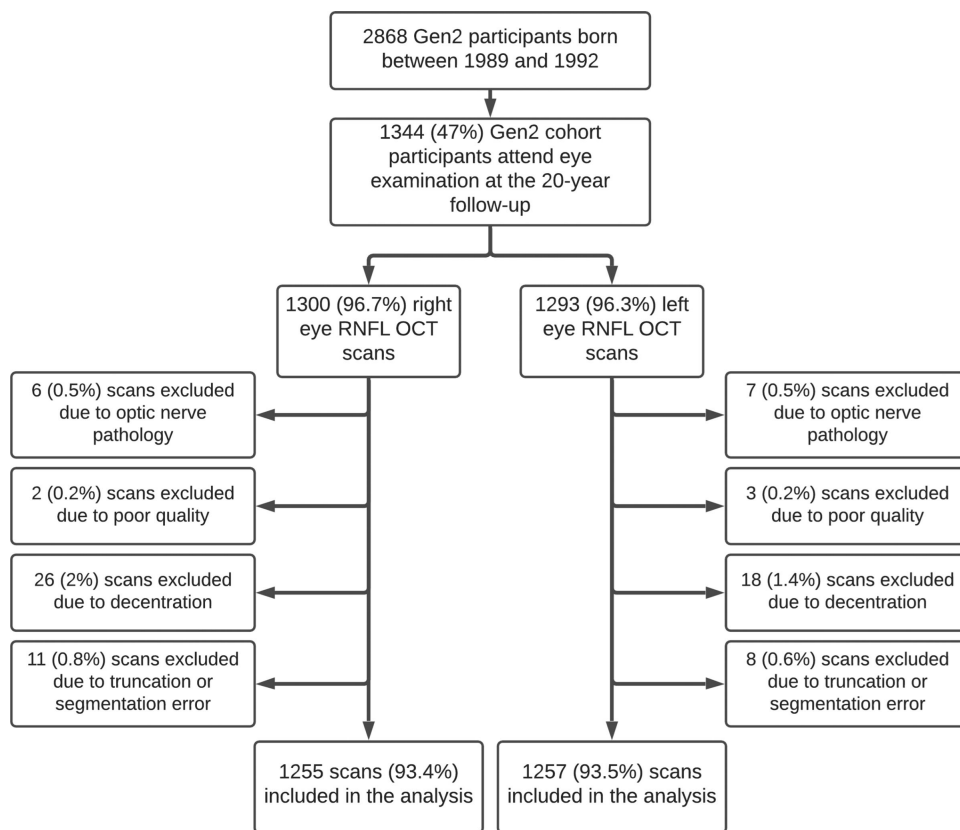


Figure 1. Flow diagram showing recruitment for the Generation 2 cohort of the Raine Study and number and reasons OCT scans of the peripapillary RNFL were excluded.

Table 1. Participant Characteristics

Demographics	Raine Study Gen2 (n = 1288)
Female, n (%)	626 (48.6)
Age, mean (range), y	20.0 (19.1–22.1)
Ethnicity, n (%)	
European	1101 (85.5)
East or Southeast Asian	75 (5.8)
Other	112 (8.7)
Height, mean (SD), m	1.73 (0.10)
Weight, mean (SD), kg	73.1 (17.1)
Axial length, mean (SD), mm	23.60 (0.92)
Spherical equivalent, median (IQR), D	0.25 (−0.38, 0.63)
Myopia, ^a n (%)	260 (20.5)
Intraocular pressure, mean (SD), mm Hg	15.4 (3.43)

^aMyopia defined as mean spherical equivalent of both eyes < −0.50 diopters.

different between the European ancestry and “other” ancestry groups, but the East or Southeast Asian ancestry group had slightly thicker temporal RNFL and thinner nasal RNFL compared to the European ancestry group. Higher IOP was associated with a

thinner RNFL at the inferonasal sector, and self-reported cigarette smoking was associated with thinner temporal RNFL. Axial length was strongly associated with RNFL thickness being associated with a thicker temporal RNFL and thinner RNFL in all other

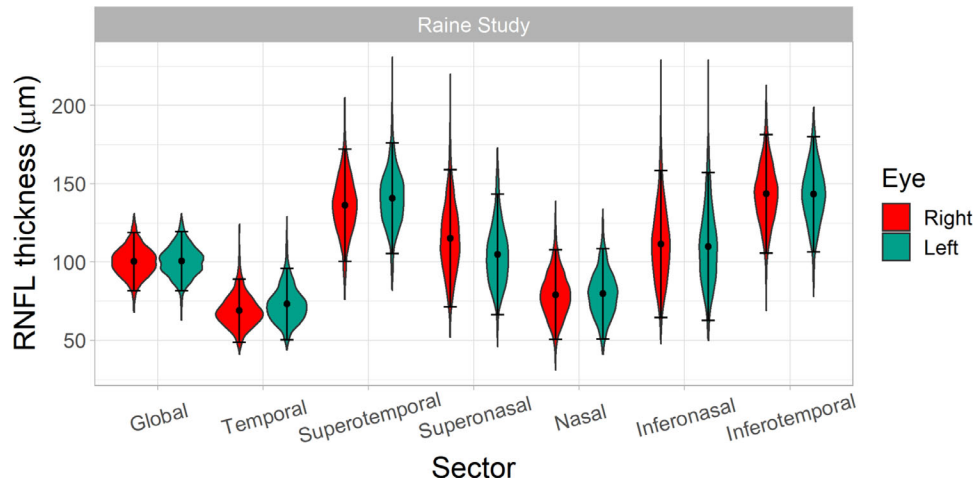


Figure 2. Violin plots showing distributions of peripapillary RNFL thickness in the global and in each of the six RNFL sectors in the right and left eyes of Generation 2 Raine Study participants, separately. Right eye data are shown in *blue* and left eye data in *red*. The points represent the mean RNFL thicknesses and error bars represent ± 1.96 standard deviations from the mean.

Table 2. Descriptive Statistics of RNFL Thickness in Each of Sector for Both Eyes Combined and Right and Left Eyes Separately

Sector	Both Eyes		Right Eye		Left Eye		P Value ^a
	Mean (SD)	First, Fifth Centiles	Mean (SD)	First, Fifth Centiles	Mean (SD)	First, Fifth Centiles	
Global (µm)	100.0 (9.6)	78, 85	100.5 (9.7)	78, 85	100.3 (9.5)	78, 85	0.03
Temporal (µm)	71.0 (11.1)	45, 53	73.1 (11.6)	46, 54	68.9 (10.3)	45, 52	<0.001
Superotemporal (µm)	138.5 (18.3)	96, 108	140.6 (18.0)	99, 111	136.3 (18.3)	94, 106	<0.001
Superonasal (µm)	110.0 (21.6)	60, 74	104.9 (19.6)	59, 72	115.1 (22.3)	63, 78	<0.001
Nasal (µm)	79.4 (14.6)	45, 55	79.7 (14.7)	46, 55	79.1 (14.6)	45, 55	0.09
Inferonasal (µm)	110.6 (24.0)	55, 71	109.8 (24.1)	54, 70	111.5 (24.0)	56, 72	<0.001
Inferotemporal (µm)	143.4 (19.0)	100, 112	143.2 (18.8)	100, 112	143.6 (19.3)	99, 112	0.51

^aFor test of the null hypothesis that RNFL thickness is the same in the right and left eyes calculated using linear mixed model with random intercepts to account for correlation between eyes. A Bonferroni correction was applied due to multiple testing and $P < 0.007$ is considered statistically significant. Data from all 1288 participants in the analysis were included.

sectors. After adjusting for axial length, IOP was no longer associated with inferonasal RNFL thickness ($P = 0.03$), and East or Southeast Asian ethnicity was no significantly associated with global or nasal RNFL thickness ($P > 0.05$). After adjusting for axial length, male sex remained significantly associated with thinner temporal (mean difference = -2.66 ; 95% CI, -3.79 to -1.54) and inferotemporal RNFL (mean difference = -3.05 ; 95% CI, -5.03 to -1.07), and cigarette smoking remained significantly associated with thinner temporal RNFL (mean difference = -3.61 ; 95% CI, -5.49 to -1.74). RNFL thickness data (mean, SD, centiles) stratified by emmetropic, myopic, and hyperopic status are displayed in Supplementary Figure S1 and Supplementary Table S2.

Classification of RNFL Thickness

After matching the characteristics of our study participants to those of the Heidelberg Spectralis normative database (i.e., includes those of northern European ancestry, IOP ≤ 22 mm Hg and spherical equivalent ≥ -7 D and $\leq +5$ D), 1050 (81.5%) participants remained in the analysis. Of these participants, 69.9% (734) had WNL classifications in all sectors of both eyes. Therefore, approximately one-quarter of participants had a BL or ONL classification in one or both eyes.

The percentages of BL and ONL classifications in right and left eyes are shown in Figure 3. The error bars represent 99.3% CIs (in line with a Bonferroni

Table 3. Unadjusted Associations between RNFL Thickness in the Various RNFL Sectors and Demographic and Ocular Characteristics

Characteristic	Age, y	Sex ^a	Ethnicity: East or Southeast Asian vs. European ^b		Ethnicity: Other Ethnicity vs. European ^b		Axial Length (mm)	IOP (mm Hg)	Smoking
			Estimate	P	Estimate	P			
G	-1.29 (-2.42, -0.17) P = 0.02	-1.21 (-2.34, -0.18) P = 0.02	-5.27 (-8.43, -2.11) P = 0.001	0.70	-0.39 (-3.01, 2.23) P = 0.77	-2.69 (-3.16, -2.22) P < 0.001	-0.05 (-0.14, 0.03) P = 0.22	-0.35 (-2.11, 1.42) P = 0.70	
T	-1.32 (-2.53, -0.11) P = 0.03	-1.74 (-2.84, -0.64) P = 0.002	2.52 (0.16, 4.88) P = 0.04	-3.18 (-3.46, 0.46) P = 0.13	1.74 (1.15, 2.33) P < 0.001	0.14 (-0.01, 0.28) P = 0.06	-3.80 (-5.79, -1.92) P < 0.001		
TS	-1.41 (-3.43, 0.60) P = 0.17	-1.65 (-3.49, 0.20) P = 0.08	3.57 (-1.00, 8.15) P = 0.13	-3.18 (-6.46, 0.09) P = 0.06	-2.30 (-3.28, -1.33) P < 0.001	0.06 (-0.17, 0.30) P = 0.59	-0.93 (-4.05, 2.19) P = 0.56		
NS	-2.35 (-4.69, -0.02) P = 0.05	-1.49 (-3.63, 0.65) P = 0.17	0.54 (-0.94, 2.02) P = 0.47	0.34 (-3.46, 4.14) P = 0.86	-3.93 (-5.05, -2.80) P < 0.001	-0.40 (-0.68, -0.12) P = 0.005	2.57 (-1.07, 6.22) P = 0.17		
N	-0.52 (-2.14, 1.09) P = 0.53	0.54 (-0.94, 2.02) P = 0.47	-5.27 (-8.43, -2.11) P = 0.001	-0.39 (-3.01, 2.23) P = 0.77	-4.05 (-4.81, -3.29) P < 0.001	-0.08 (-0.27, 0.10) P = 0.10	1.48 (-1.05, 4.01) P = 0.25		
NI	-1.37 (-4.07, 1.33) P = 0.32	-0.40 (-2.87, 2.07) P = 0.75	-2.28 (-7.56, 3.00) P = 0.40	1.05 (-3.34, 5.43) P = 0.64	-7.13 (-8.38, -5.88) P < 0.001	-0.44 (-0.73, -0.15) P = 0.003	3.45 (-0.77, 7.66) P = 0.11		
TI	-1.57 (-3.69, 0.56) P = 0.15	-4.10 (-6.03, -2.17) P < 0.001	0.53 (-3.62, 4.68) P = 0.80	-3.84 (-7.29, -0.39) P = 0.03	-2.60 (-3.63, -1.58) P < 0.001	-0.17 (-0.40, 0.07) P = 0.17	-2.95 (-6.26, 0.36) P = 0.08		

Linear mixed models were used to analyze associations. A random intercepts term was included for participants to account for correlation between eyes. Values represent the average change in RNFL thickness (µm) in each sector (row headings) for each 1-unit increase in the explanatory variables (column headings). Values in brackets show the 95% confidence intervals for the estimate, and P values are shown after the 95% confidence intervals. Bold values are significant with the Bonferroni correction (P < 0.007). G, global; N, nasal; NI, inferonasal; NS, superonasal; T, temporal; TI, inferotemporal; TS, superotemporal.

^aFemale sex is the reference group.

^bEuropean ethnicity is the reference group.

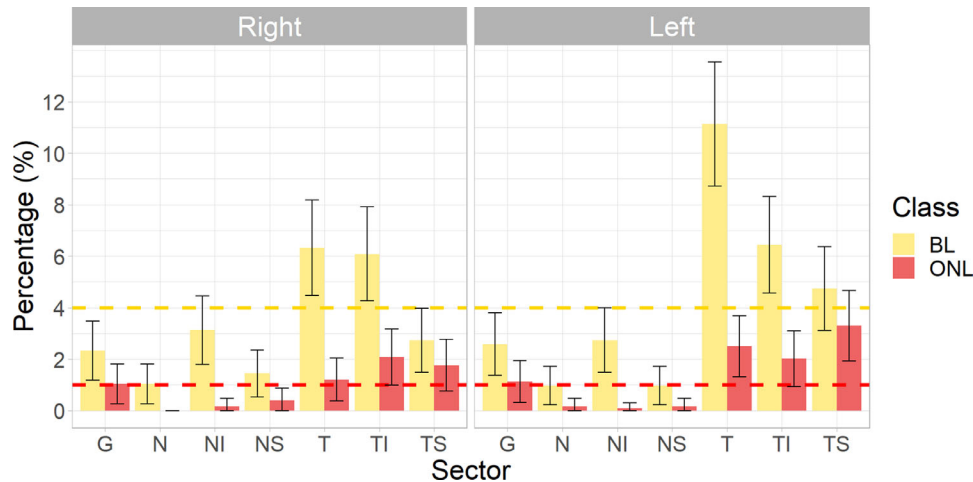


Figure 3. Percentage of BL and ONL classifications in the global (G), nasal (N), inferonasal (NI), superonasal (NS), temporal (T), inferotemporal (TI), and superotemporal (TS) RNFL sectors of the right and left eyes of 1050 Generation 2 Raine Study participants who were of Northern European ancestry, had a spherical equivalent between -7 and $+5$ dioptres and had an intraocular pressure less than or equal to 22 mmHg. The expected percentages are 4% for BL classifications and 1% for ONL classifications in all sectors. The error bars represent the 99.3% CIs (in line with the Bonferroni correction) for the estimated prevalence of each of the classifications in each sector. If the error bar does not cross the expected prevalence of 4% and 1% for BL and ONL classifications, respectively, then the prevalence of the BL or ONL classification is significantly different from the manufacturer database.

corrected), and if not crossing the expected value of 4% or 1% for BL and ONL, respectively, then the prevalence is significantly different from the expected value. For the global RNFL sector, there was a lower than expected prevalence of BL classifications for both the right (2.3%) and left (2.6%) eyes, but the prevalence of ONL classifications was not significantly different from the expected prevalence of 1% in either eye. There was a higher than expected frequency of BL classification in the temporal and inferotemporal sectors of both eyes and a lower than expected frequency of BL classifications in the global, nasal, and superonasal sectors of both eyes. The prevalence of BL classifications in the superotemporal sector was lower than expected in the right eye and higher than expected in the left eye. We found higher than expected frequencies of ONL classification in the inferotemporal and superotemporal sectors of the right eye and in the temporal, inferotemporal, and superotemporal sectors of the left eye. ONL classifications were lower than expected for all nasal sectors of both eyes. We applied the first and fifth centile cutoffs derived based on this study (shown in Table 2) to develop new RNFL thickness classifications and compared these to the manufacturer classifications in Supplementary Table S3. All participants were included in the analysis for this comparison as the mean and centiles were derived from the entire study sample. Weighted κ statistics for agreement between the classifications derived from this study and manufac-

turer classifications were global = 0.75, temporal = 0.49, superotemporal = 0.98, superonasal = 0.85, nasal = 0.22, inferonasal = 0.95, and inferotemporal = 0.68 (all $P < 0.001$) for right eyes and global = 0.77, temporal = 0.26, superotemporal = 0.61, superonasal = 0.40, nasal = 0.30, inferonasal = 0.86, and inferotemporal = 0.64 (all $P < 0.001$) for left eyes. Agreement was poorest for the temporal sector of the left eye and nasal sectors of the right and left eyes, in keeping with data shown in Figure 3.

Interocular symmetry in RNFL classification is investigated in Table 4, which shows frequency of WNL, BL and ONL classifications in the right versus left eye for all participants. A high proportion of participants had a classification of WNL in both eyes due to the higher probability (0.95) of a WNL classification. Weighted κ statistics for agreement between right and left eyes were global = 0.67, temporal = 0.36, superotemporal = 0.28, superonasal = 0.34, nasal = 0.39, inferonasal = 0.41, and inferotemporal = 0.36 (all $P < 0.001$). These weighted κ statistics take into account this chance agreement due to a higher probability of a WNL classification and indicate that the high proportion of participants having WNL classifications in both eyes is in part due to the high probability of a WNL classification. Interocular symmetry in RNFL classification was greatest in the global sector, whereas the superotemporal sector was the most asymmetrical in RNFL thickness classification.

Table 4. Frequency Tables Comparing WNL, BL, and ONL RNFL Thickness Classifications in the Right and Left Eyes of Raines Study Participants

All Sectors	Left Eye Classification, n (%)				Right Eye Classification				Left Eye Classification, n (%)				
	WNL	BL	ONL	Total	WNL	BL	ONL	Total	WNL	BL	ONL	Total	
Right eye classification	WNL 7809 (92.8)	224 (2.7)	41 (0.5)	8074 (95.9)	Right eye classification	WNL 1149 (95.8)	15 (1.3)	0 (0)	1164 (97.0)	WNL 1090 (90.5)	42 (3.5)	21 (1.7)	1153 (95.8)
	BL 131 (1.6)	101 (1.2)	35 (0.4)	267 (3.2)		BL 6 (0.5)	15 (1.3)	4 (0.3)	25 (2.1)	BL 7 (0.6)	7 (0.6)	10 (0.8)	32 (1.3)
	ONL 14 (0.2)	28 (0.3)	35 (0.4)	77 (0.9)		ONL 0 (0)	1 (0.1)	10 (0.8)	11 (0.9)	ONL 7 (0.6)	7 (0.6)	7 (0.6)	19 (0.8)
	Total 1954 (94.5)	353 (4.2)	111 (1.3)	8418 (100)		Total 1155 (96.3)	31 (2.6)	14 (1.2)	1200 (100)	Total 1110 (92.2)	56 (4.7)	38 (3.2)	1204 (100)
T	WNL	BL	ONL	Total	TS	WNL	BL	ONL	Total	WNL	BL	ONL	Total
Right eye classification	WNL 1008 (83.9)	92 (7.7)	10 (0.8)	1110 (92.4)	Right eye classification	WNL 1090 (90.5)	42 (3.5)	21 (1.7)	1153 (95.8)	WNL 1090 (90.5)	42 (3.5)	21 (1.7)	1153 (95.8)
	BL 29 (2.4)	35 (2.9)	13 (1.0)	77 (3.1)		BL 15 (1.2)	7 (0.6)	10 (0.8)	32 (1.3)	BL 7 (0.6)	7 (0.6)	7 (0.6)	19 (0.8)
	ONL 1 (0.1)	5 (0.4)	8 (0.7)	14 (0.6)		ONL 5 (0.4)	7 (0.6)	7 (0.6)	19 (0.8)	ONL 7 (0.6)	7 (0.6)	7 (0.6)	19 (0.8)
	Total 1038 (86.4)	132 (11.0)	31 (2.6)	1201 (100)		Total 1110 (92.2)	56 (4.7)	38 (3.2)	1204 (100)	Total 1110 (92.2)	56 (4.7)	38 (3.2)	1204 (100)
NS	WNL	BL	ONL	Total	N	WNL	BL	ONL	Total	WNL	BL	ONL	Total
Right eye classification	WNL 1177 (97.7)	6 (0.5)	1 (0.1)	1184 (98.3)	Right eye classification	WNL 1181 (98.3)	7 (0.6)	2 (0.2)	1190 (99.1)	WNL 1181 (98.3)	7 (0.6)	2 (0.2)	1190 (99.1)
	BL 12 (1.0)	4 (0.3)	0 (0)	16 (0.6)		BL 6 (0.5)	5 (0.4)	0 (0)	11 (0.4)	BL 5 (0.4)	5 (0.4)	0 (0)	11 (0.4)
	ONL 2 (0.2)	2 (0.2)	1 (0.1)	5 (0.2)		ONL 0 (0)	0 (0)	0 (0)	0 (0)	ONL 0 (0)	0 (0)	0 (0)	0 (0)
	Total 1191 (98.8)	12 (1.0)	2 (0.2)	1205 (100)		Total 1187 (98.8)	12 (1.0)	2 (0.2)	1201 (100)	Total 1187 (98.8)	12 (1.0)	2 (0.2)	1201 (100)
NI	WNL	BL	ONL	Total	TI	WNL	BL	ONL	Total	WNL	BL	ONL	Total
Right eye classification	WNL 1149 (95.5)	16 (1.3)	0 (0)	1165 (96.8)	Right eye classification	WNL 1055 (87.6)	46 (3.8)	7 (0.6)	1108 (92.0)	WNL 1055 (87.6)	46 (3.8)	7 (0.6)	1108 (92.0)
	BL 22 (1.8)	14 (1.2)	0 (0)	36 (1.4)		BL 41 (3.4)	21 (1.7)	8 (0.7)	70 (2.8)	BL 41 (3.4)	21 (1.7)	8 (0.7)	70 (2.8)
	ONL 0 (0)	2 (0.2)	0 (0)	2 (0.1)		ONL 6 (0.5)	11 (0.9)	9 (0.7)	26 (1.0)	ONL 6 (0.5)	11 (0.9)	9 (0.7)	26 (1.0)
	Total 1171 (97.3)	31 (2.7)	0 (0)	1203 (100)		Total 1102 (91.5)	78 (6.5)	24 (2.0)	1204 (100)	Total 1102 (91.5)	78 (6.5)	24 (2.0)	1204 (100)

Data are shown for all sectors combined and individually for each RNFL sector. Percentages are calculated by dividing the number of occurrences by the grand total. All 1288 participants were included for this comparison.

Discussion

We report the distribution of peripapillary RNFL thickness in a young, healthy population of Australian adults. When data from both eyes were combined, the global RNFL thickness was similar to that of 17-year-old Australians in the Sydney Adolescent and Vascular Eye Study (SAVES; 100.5 μm vs. 99.4 μm), as was the mean temporal RNFL thickness (71.0 μm vs. 69.9 μm), but the mean nasal RNFL was slightly thicker in this study (79.4 μm vs. 74.3 μm).⁴ The SAVES used a Cirrus HD-OCT 4000 (Carl Zeiss, Jena, Germany), which may explain some of these slight differences. Published studies have examined predominantly older age groups, and studies in Germany, Singapore, and the United States all identified thinner average RNFL than found in this study,^{6,17,18} in keeping with the known association between older age and thinner RNFL.^{6,19} However, studies conducted in China,⁵ India,²⁰ and South Africa³ found slightly thicker mean RNFL (102 μm , 104.8 μm , and 108.7 μm , respectively) compared to this study. The South African study excluded participants with axial length >26 mm, which may partly explain the much thicker RNFL in their study.

Axial length had a substantial impact on RNFL, with longer axial length being associated with thinner RNFL in all sectors except the temporal sectors, in which longer axial length was associated with thicker RNFL. The relationship between axial length and RNFL has been previously described, and studies^{11,21} have shown that this largely occurred due to the effect of axial length-related ocular magnification on the diameter of the OCT circle scan.²¹ The circle scan should have a diameter of 3.4 mm, but the actual diameter of the circle scan (in mm) is larger in longer eyes and smaller in shorter eyes. Thus, in longer eyes, the RNFL thickness is measured further away from the optic nerve head (as illustrated in Supplementary Fig. S2). This leads to a thinner RNFL measurement because the RNFL is naturally thinner further away from the optic nerve, where the nerve fibers are spread over a greater area.²² Yoo and colleagues²³ also demonstrated that with increasing axial length, the position of the thicker superior and inferior RNFL bundles tends to shift temporally, thus increasing the mean RNFL thickness in this sector and explaining the relationship between longer axial length and thicker temporal RNFL. We were not able to adjust circle scan diameter for axial length in this analysis, but this also means our findings are applicable to the clinical setting.

There were significant differences in RNFL thicknesses between eyes in this population. Compared to

the left eye, the right eye peripapillary RNFL was thicker in the temporal and superotemporal sectors and thinner in the superonasal sector. The weighted κ analysis showed that symmetry between the two eyes was poorest in the superotemporal sector ($\kappa = 0.28$). This finding is in line with previous studies that have noted that right eye superior RNFL is generally thinner than in the left eye and temporal RNFL generally thicker.^{7,24,25} This phenomenon has been explained by asymmetry in the positioning of the superior retinal artery, vein, and nerve fiber bundle between eyes, being located more slightly temporally in right eyes compared to left eyes,^{7,24,26} thus contributing to a thicker temporal RNFL and thinner superior RNFL in right eyes. Interestingly, agreement between right and left eye classification was much higher in the global sector ($\kappa = 0.67$) compared to all other sectors, suggesting that the placement of the boundaries to define other RNFL boundaries (i.e., temporal, nasal, etc.) is contributing to interocular asymmetry in classification. While differences in RNFL thickness between eyes were statistically significant, the mean differences in RNFL thickness were generally small, particularly for the global, nasal, and inferonasal sectors, and may not be clinically relevant. Nevertheless, these small differences impact the prevalence of ONL and BL classifications, as shown in Figure 3, and thus manufacturers should consider developing right eye- and left eye-specific reference databases for RNFL thickness.

Unlike previous studies,^{3,6,27} we did not find any substantial impacts of ethnicity on RNFL thickness in this study. Compared to those of European ancestry, participants of East and Southeast Asian ancestry had thicker temporal RNFL and thinner nasal RNFL, but this was largely explained by differences in axial length between the groups. There was no significant difference in RNFL thickness between the European ancestry group and the “other” ancestry group. This may be due to the relatively diverse range of ethnicities of participants who were included in the “other” ethnicity group; however, we were not able to divide these participants into more meaningful ethnic groups. The number of participants of non-European ethnicity was also relatively small and may explain why we did not find any significant difference between groups. Males in this study generally had thinner measured RNFL than females, and this was particularly evident in the temporal and superotemporal sectors. We also identified that smoking cigarettes was associated with thinner temporal RNFL after adjusting for axial length. Maternal smoking during pregnancy has been associated with thinner peripapillary RNFL, but current smoking has been associated with thinner RNFL⁵ or thicker RNFL²⁸ or found not to be significantly associated

with RNFL thickness.²⁹ As only temporal RNFL thickness was associated with smoking, we conclude that there is only weak evidence of an association in this study.

We found that the frequency of BL and ONL RNFL classifications from the SD-OCT used in this study was higher than expected in the temporal sectors and lower than expected in the nasal sectors. This was further reiterated by the poorer agreement between the manufacturer reference database and the RNFL thickness classifications derived from the current study in the temporal and nasal sectors of the right and left eyes. As longer axial length is associated with thicker temporal RNFL but thinner nasal RNFL (when not corrected for ocular magnification effects),¹¹ we suspect that our study sample had a shorter axial length on average compared to the reference database. Although the characteristics of the Heidelberg Spectralis reference group are reported in the manual ($n = 201$, 111 [55%] males, mean age = 48.2 years, age range = 18–78 years), data on axial length are not published for this cohort, and we are therefore unable to test this. The higher proportion of males, who had thinner temporal and superotemporal RNFL in this study, could explain some of the differences in RNFL distribution between this study and the OCT manufacturer database. The higher frequency of BL and ONL classifications in the temporal and superotemporal sectors of the left eye, compared to the right eye, is in keeping with the interocular asymmetry noted in this and previous studies.^{7,25} The Heidelberg Spectralis and other OCT manufacturer databases do not use eye-specific cutoffs for BL and ONL classifications,²⁴ which are needed to account for interocular asymmetry. Fovea to disc angle and the subsequent placement of boundaries defining RNFL sectors around the optic disc (e.g., temporal, nasal) also impact sectoral, but not global, RNFL thickness measurements. In this study, the manufacturer software identified the fovea during acquisition of RNFL scans by ascertaining the location on the retina that is being used to fix on the fixation target. However, eccentric or poor fixation would lead to changes in the placement of RNFL sectoral boundaries and subsequent calculations of sectoral RNFL thicknesses. Global RNFL thickness is independent of the placement of RNFL sectoral boundaries, and we identified that the prevalence of BL classifications in global sectors was lower than expected in both eyes, indicating that our results may be independent of fovea to disc angle.

Our study has some novel and clinically meaningful findings. First, this study presented the distribution of RNFL thickness in a large young adult population. While young adults are not at high risk of glaucoma,

glaucoma can present at any age, and it is becoming more common for this population to undergo routine RNFL OCT scans. Thus, it is important to establish the expected distribution of RNFL thickness in a healthy, young adult population to enable early identification of glaucoma in this age group. Second, when we applied the inclusion/exclusion criteria used in the manufacturer database—with the exception of normal visual fields—our study found that the OCT manufacturer database misclassified RNFL thicknesses in this young adult cohort. As OCT technology becomes more widely available, it is crucial for eye care providers to be aware of the limitations of reference databases. Reference databases themselves could be improved by accounting for eye laterality (i.e., right versus left eyes) and axial length.

Clinicians should be aware that individuals who are hyperopic and have a shorter axial length are likely to have a thinner temporal RNFL and a thicker nasal RNFL, whereas individuals with longer axial lengths are likely to have a thinner RNFL in all sectors except the temporal RNFL, which will be thicker. In this healthy population, we demonstrated that RNFL thickness profiles were different between the two eyes but that classifications were still somewhat symmetrical between the right and left eyes. We also showed that, despite the rarity of glaucoma in young adults, it is quite common for RNFL values to fall outside the normal range in this population. Therefore, a single RNFL thickness measurement is likely not a good predictor of glaucoma, and the results of a full glaucoma workup should be considered when diagnosing glaucoma.

Limitations of this study are that we were not able to adjust the RNFL circle scan diameter for axial length or account for anatomic factors such as optic nerve head size and the position and density of blood vessels around the optic nerve head, which can impact RNFL thickness.³⁰ However, these factors are typically not accounted for in clinical practice, and thus our results are applicable to the clinical setting. The results describing RNFL thickness in this population may not be generalizable to patients who are of a different age, have a scan with a Q quality score <20, or for whom corneal curvature values are not available. We also only relied on examiner judgment to determine whether RNFL circle scans were centered, and minor deviations from center could have contributed to some of our findings. Visual field testing was not performed, and participants with subclinical eye diseases or visual field defects were not excluded from this analysis. This is unlikely to have had a considerable impact on our results because subclinical disease or visual field defects are likely to be rare in this population. However, it

does mean that we were unable to exactly replicate the manufacturer reference database, which only included people with normal visual fields. Additionally, we are unsure if the Heidelberg proprietary database inputs corneal curvature, and this may be another point of difference between this study and the reference database. It is also possible that optic disc size and mean fovea-to-disc angle differed between the current study and the manufacturer reference database. However, we were unable to assess this as the information was not available from the manufacturer. Last, the Raine Study is not a population-based study. The Gen2 cohort has been shown to be relatively, but not entirely, representative of the Western Australian population.¹⁴ Thus, it is possible that the distributions of RNFL presented in this study may not be exactly representative of the wider population. Strengths of this study are the large sample size, high proportion of participants with complete SD-OCT data, and relatively representative sample.

We describe the normal distribution of RNFL thickness in a sample of Australian young adults, a population in whom very little normal data are available. The frequency of ONL and BL classifications was overrepresented in temporal sectors and underrepresented in nasal sectors. Furthermore, ONL and BL classifications were more common in the left eyes than in right eyes. Clinicians should be aware of the known interocular asymmetry in RNFL thickness profiles, the impact of axial length on measured RNFL thickness, and the potential limitations of OCT manufacturer reference databases. More reference data are required to better define the normal variation in RNFL thickness in different populations.

Acknowledgments

The authors thank the staff, participants, and funders of the Raine Study

Supported by the University of Western Australia (UWA), The Telethon Kids Institute, Raine Medical Research Foundation, Women and Infants Research Foundation, Curtin University, Edith Cowan University, Murdoch University, and the University of Notre Dame Australia. The eye examination was funded by grants from the National Health and Medical Research Council (NHMRC) Project Grants (1021105), Lions Eye Institute, the Australian Foundation for the Prevention of Blindness, Alcon Research Institute, Ophthalmic Research Institute of Australia (ORIA), and Telethon.

The funding organization had no role in the design or conduct of this research.

Disclosure: **G. Lingham**, None; **S.S.-Y. Lee**, None; **J. Charng**, None; **A. Clark**, None; **F.K. Chen**, None; **S. Yazar**, None; **D.A. Mackey**, None

References

- Schuman JS, Hee MR, Puliafito CA, et al. Quantification of nerve fiber layer thickness in normal and glaucomatous eyes using optical coherence tomography: a pilot study. *Arch Ophthalmol*. 1995;113:586–596.
- Weinreb RN, Aung T, Medeiros FA. The pathophysiology and treatment of glaucoma: a review. *JAMA*. 2014;311:1901–1911.
- Ismail S, Ally N, Alli HD. Retinal nerve fibre layer thickness in a normal black South African population. *Eye*. 2020;34:1426–1431.
- Tariq YM, Li H, Burlutsky G, Mitchell P. Retinal nerve fiber layer and optic disc measurements by spectral domain oct: normative values and associations in young adults. *Eye (London)*. 2012;26:1563–1570.
- Zhao L, Wang Y, Chen CX, Xu L, Jonas JB. Retinal nerve fibre layer thickness measured by spectralis spectral-domain optical coherence tomography: the Beijing Eye Study. *Acta Ophthalmol Scand*. 2014;92:e35–41.
- Ho H, Tham YC, Chee ML, et al. Retinal nerve fiber layer thickness in a multiethnic normal Asian population: the Singapore Epidemiology of Eye Diseases Study. *Ophthalmology*. 2019;126:702–711.
- Wagner FM, Hoffmann EM, Nickels S, et al. Peripapillary retinal nerve fiber layer profile in relation to refractive error and axial length: results from the Gutenberg Health Study. *Transl Vis Sci Technol*. 2020;9:35–35.
- Dolgin E. The myopia boom. *Nature*. 2015;519:276–278.
- Williams KM, Bertelsen G, Cumberland P, et al. Increasing prevalence of myopia in Europe and the impact of education. *Ophthalmology*. 2015;122:1489–1497.
- Kang M-T, Li S-M, Li H, et al. Peripapillary retinal nerve fibre layer thickness and its association with refractive error in Chinese children: the Anyang Childhood Eye Study. *Clin Exp Ophthalmol*. 2016;44:701–709.
- Kang SH, Hong SW, Im SK, Lee SH, Ahn MD. Effect of myopia on the thickness of the retinal

- nerve fiber layer measured by Cirrus HD optical coherence tomography. *Invest Ophthalmol Vis Sci.* 2010;51:4075–4083.
12. Haarman AEG, Enthoven CA, Tideman JW, Tedja MS, Verhoeven VJM, Klaver CCW. The complications of myopia: a review and meta-analysis. *Invest Ophthalmol Vis Sci.* 2020;61:49.
 13. Yazar S, Forward H, McKnight CM, et al. Raine Eye Health Study: design, methodology and baseline prevalence of ophthalmic disease in a birth-cohort study of young adults. *Ophthalmic Genet.* 2013;34:199–208.
 14. Straker L, Mountain J, Jacques A, et al. Cohort profile: the Western Australian Pregnancy Cohort (Raine) Study—Generation 2. *Int J Epidemiol.* 2017;46:1384–1385j.
 15. Chung HK, Han YK, Oh S, Kim SH. Comparison of optical coherence tomography measurement reproducibility between children and adults. *PLoS ONE.* 2016;11:e0147448.
 16. Tewarie P, Balk L, Costello F, et al. The OSCAR-IB consensus criteria for retinal oct quality assessment. *PLoS ONE.* 2012;7:e34823.
 17. Alasil T, Wang K, Keane PA, et al. Analysis of normal retinal nerve fiber layer thickness by age, sex, and race using spectral domain optical coherence tomography. *J Glaucoma.* 2013;22:532–541.
 18. Bendschneider D, Tornow RP, Horn FK, et al. Retinal nerve fiber layer thickness in normals measured by spectral domain oct. *J Glaucoma.* 2010;19:475–482.
 19. Alamouti B, Funk J. Retinal thickness decreases with age: an OCT study. *Br J Ophthalmol.* 2003;87:899–901.
 20. Ramakrishnan R, Mittal S, Ambatkar S, Kader M. Retinal nerve fibre layer thickness measurements in normal Indian population by optical coherence tomography. *Indian J Ophthalmol.* 2006;54:11–15.
 21. Savini G, Barboni P, Parisi V, Carbonelli M. The influence of axial length on retinal nerve fibre layer thickness and optic-disc size measurements by spectral-domain OCT. *Br J Ophthalmol.* 2012;96:57–61.
 22. Iester M, Mermoud A. Normal retinal nerve fiber layer thickness in the peripapillary region measured by scanning laser polarimetry. *J Glaucoma.* 2001;10(3):170–176.
 23. Yoo YC, Lee CM, Park JH. Changes in peripapillary retinal nerve fiber layer distribution by axial length. *Optom Vis Sci.* 2012;89:4–11.
 24. Cameron JR, Megaw RD, Tatham AJ, et al. Lateral thinking—interocular symmetry and asymmetry in neurovascular patterning, in health and disease. *Prog Retin Eye Res.* 2017;59:131–157.
 25. Dalglish JD, Tariq YM, Burlutsky G, Mitchell P. Symmetry of retinal parameters measured by spectral-domain oct in normal young adults. *J Glaucoma.* 2015;24:20–24.
 26. Hwang YH, Song M, Kim YY, Yeom DJ, Lee JH. Interocular symmetry of retinal nerve fibre layer thickness in healthy eyes: a spectral-domain optical coherence tomographic study. *Clin Exp Optom.* 2014;97:550–554.
 27. Samarawickrama C, Wang JJ, Huynh SC, et al. Ethnic differences in optic nerve head and retinal nerve fibre layer thickness parameters in children. *Br J Ophthalmol.* 2010;94:871–876.
 28. Mauschitz MM, Bonnemaier PWM, Diers K, et al. Systemic and ocular determinants of peripapillary retinal nerve fiber layer thickness measurements in the European eye epidemiology (e3) population. *Ophthalmology.* 2018;125:1526–1536.
 29. Rougier M-B, Korobelnik J-F, Malet F, et al. Retinal nerve fibre layer thickness measured with SD-OCT in a population-based study of French elderly subjects: the Alienor Study. *Acta Ophthalmol.* 2015;93:539–545.
 30. Chua J, Schwarzhans F, Nguyen DQ, et al. Compensation of retinal nerve fibre layer thickness as assessed using optical coherence tomography based on anatomical confounders. *Br J Ophthalmol.* 2020;104:282–290.